Hindawi
Mathematical Problems in Engineering
Volume 2022, Article ID 6240165, 14 pages
https://doi.org/10.1155/2022/6240165

Research Article

State Estimation and Attack Reconstruction of Picking Robot for a Cyber-Physical System

Xu Dong,[1,2] **Zehe Wang**,[1] **and Shenghui Guo**[3]

[1]*College of Mechanical and Electrical Engineering, Hebei Agricultural University, Baoding 071000, China*
[2]*College of Mechanical and Electrical Engineering, North China Institute of Aerospace Engineering, Langfang 065000, China*
[3]*College of Electronics and Information Engineering, Suzhou University of Science and Technology, Suzhou 215009, China*

Correspondence should be addressed to Zehe Wang; zehewang@hebau.edu.cn

Received 9 June 2022; Revised 12 October 2022; Accepted 31 October 2022; Published 23 November 2022

Academic Editor: Ha Quang Thinh Ngo

A novel method based on the unknown input observer is proposed to reconstruct sensor attacks and estimate system states for fruit and vegetable picking robot cyber-physical systems. By fully considering the nonlinear characteristics of the articulated fruit and vegetable picking robot system as well as the influences of external disturbances, the generalized system model is established and the unknown input observer is designed to reduce false positives and false negatives in the agricultural cyber-physical system. In view of the agricultural production environment, a digital prototype model is established for manipulators of picking robot with three joints. Following the Lagrange method, dynamic equations of the manipulator system are established and transformed into a corresponding state-space model, where the nonlinearity and unknown input information are taken into account. Then, the original system is converted into a generalized system through state augmentations based on the generalized system theory. Furthermore, an H_∞ unknown input observer is designed to estimate the system state and reconstruct sensor attacks, accommodating nonlinear characteristics and external disturbance effects of the system. The asymptotic stability of the dynamic error system is proved via the Lyapunov function. By simulation and comparison with an existing method, the results demonstrate that the proposed method reconstructs sensor attacks and estimates system states effectively.

1. Introduction

In recent years, the cyber-physical system (CPS), a novel intelligent system based on the technical integration of control, computer, and communication, has been widely used in power system [1], intelligent transportation [2], product manufacture [3], industrial control [4], etc. and has broad development prospects. Specifically, CPS technologies applied in the industrial field lay the foundation for the industrial cyber-physical system (ICPS) [5]. On the other hand, the integration of the CPS into agriculture can be referred to as the agriculture cyber-physical system (ACPS) [6], which is typified by the intelligent ACPS [7]. In addition to completing the picking task, the CPS picking robots can also collect data and feed it back to the control end through sensors to monitor the crop growth environment. CPS mobile robots are interconnected with each other, and the crop information collection becomes more reliable. Fruit and vegetable picking is a typical labor-intensive work and the most laborious link in the agricultural production chain [8].

The robot plays an important role in robot CPS, serving as a medium between information and physical world [9, 10]. The agricultural CPS robots realize the interconnection, in addition to completing the high-efficiency picking operation; they can also rely on sensors to collect data and feed it back to monitor the growth of crops. In reference to robot CPS for agricultural picking, the end of robots will directly touch fruits and vegetables, so they are usually equipped with soft fingers to protect produce from scratches, thereby improving the picking quality. Nevertheless, agricultural production features obvious timeliness and seasonality, and the working environment is complex and changeable. When multiple robots in the CPS are networked for cooperative picking works, they have to not

only tolerate impacts of environmental temperature and humidity, varying targets, obstacles, etc. but also defend network attacks for actuators and sensors in the case of frequent information exchanges [11]. Therefore, the communication network of picking robot CPS must be secured to ensure smooth implementation of picking works. Especially in busy harvest seasons, once the CPS suffers from network attacks, multiple robots may be unable to transmit accurate data information, which would directly affect the progress of agricultural production. Under the circumstances, it has great significance to figure out efficient methods on the attack detection and state estimation for picking robot CPS and to further recognize and address these attacks, so as to improve the production efficiency and promote sound development of the agricultural industry.

Notice that CPS is susceptible to network attacks and transmission errors during its operation, which will degrade the system performance. Typical attacks include data injection attack [12], denial-of-service (DoS) attack [13], and replay data attack [14]. Moreover, the wireless fading induced data package losses can also reduce the system efficiency [15]. Considering the safety of CPS, researchers have paid much attention to the detection of various attacks and proposed many effective methods. To name a few, Lee et al. [16] devised an elastic all-distribution type of state assessment scheme to protect sensors from attacks for linear dynamic systems. For the cyber-physical system under actuator and sensor attacks, Lu and Yang [17] investigated the event-triggered secure observer-based control method. In order to detect virtual data injection attacks for information physics systems, Zhao et al. [18] proposed an attack detection scheme by a subspace identification technique and verified its effectiveness based on a flight vehicle model. Hong et al. [19] proposed another attack detection method based on a residual system for industrial information physics systems. With a view to the detection of attacks from reference signals, Lucia et al. [20] took full advantage of command controller to propose a novel distributed control architecture. The fruit and vegetable picking CPS features high nonlinearity, and its actuators and sensors are susceptible to network attack signals under the influence of agricultural working environments [21–23]. Regarding CPS safety results, analytical model-based state estimation methods have constantly played a significant role, in which the observer and filter methods are the most typical, and some appealing results have been achieved [24–30]. Lu and Yang [31] Proposed a switched observer to detect attacks on sensors in information physics systems. Lv et al. [32] proposed a sliding mode observer to detect attacks on CPS. Ao et al. [33] designed an adaptive observer with online parameters to estimate attacks on states and sensors for the CPS. Palleti et al. [34] devised a fault detection method based on the Kalman filter for CPS to enhance their safety.

The abovementioned studies mainly focused on the attack detection for industrial CPS, but few results were concerned with the attack reconstruction and state estimation for the agricultural CPS. In addition, most of the attack reconstruction methods proposed in these studies are mainly adaptive observer, disturbance observer, sliding mode observer, etc. In reference to system states and sensor attack detection for the CPS of fruit and vegetable picking robots, the crux consists in determining the state vector through the dynamic model of typical joints, as well as designing the observer for sensor attack reconstruction through the state-space equation.

The main contributions of this paper are listed as follows. (1) For the first time, the sensor attack is studied for the fruit and vegetable picking robot CPS. The generalized system model is established by fully considering the nonlinear characteristics of the articulated fruit and vegetable picking robot system as well as the influences of external disturbances. (2) The unknown input observer is designed for the system state estimation and sensor attack reconstruction, and simulation verification is carried out. For the fruit and vegetable picking robot CPS, the designed observer with unknown inputs can be found to outperform those existing ones. For example, the adaptive observer proposed in [24] requires the bounded real lemma to be satisfied, while the sliding mode observer designed in [25] would give rise to discontinuous terms, hence yielding estimation results subject to vibrations. (3) A reconstruction method is proposed for system states and sensor attack of the picking robot CPS, reducing false positives and false negatives for the fault diagnosis system in agricultural harvesting equipment.

2. Dynamic Model

Modeling methods of the manipulator dynamic mainly include the Newton–Euler formula [35] and Lagrange equation [36]. For the fruit and vegetable picking manipulator, its input is the torque provided by the driving motor, and the output is the offset angle of the rod relative to the base surface or to the previous rod. Using the Lagrange equation, the closed model of a system dynamic can be established, and the relationship can be clearly described between the generalized force, generalized velocity, and generalized acceleration.

This paper considers the three-dimensional structure of a picking manipulator, as shown in Figure 1. The main components include the base, waist, big arm, forearm, and other parts, and the manipulator has six degrees of freedom. All joints in the manipulator are of rotational type, and each joint uses a servo motor as the input power source. The sensors can monitor internal states of the manipulator as well as external picking environment information. The base is fixed on a moving platform. The connecting rod between waist joints, big arm, and forearm have lengths of 50 mm, 650 mm, and 420 mm, respectively. The maximum steering angles of the waist joint, shoulder joint, and elbow joint can go up to 360 degrees, 90 degrees, and 90 degrees, respectively. Specialized picking tasks for different fruits and vegetables can be realized by refitting different types of end effectors [37].

The structure of the picking manipulator is schematically shown in Figure 2. It is assumed that the connecting rod and joint are rigid elements. The manipulator parameter is listed in Table 1.

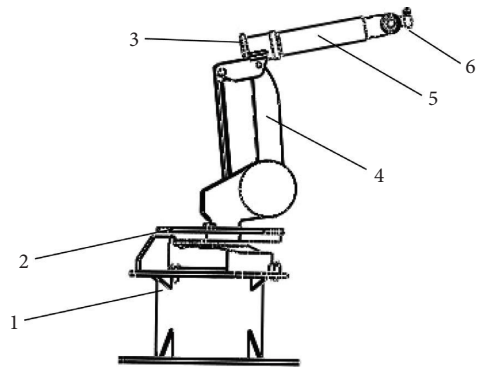

Figure 1: The structure diagram of picking robot. (1) Base, (2) waist joint, (3) shoulder joint, (4) big arm, (5) forearm, and (6) elbow.

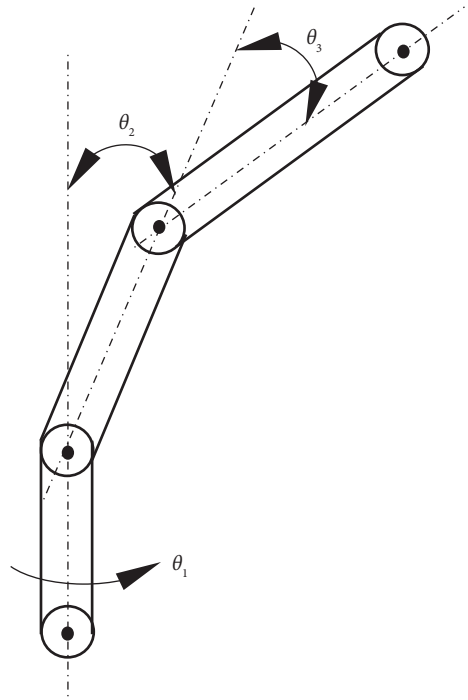

Figure 2: The configuration diagram of picking manipulators.

Table 1: Manipulator parameters.

Description	Waist joint	Big arm	Forearm
Rotation angle	θ_1	θ_2	θ_3
Length	l_1	l_2	l_3
Mass	m_{l1}	m_{l2}	m_{l3}
Moment of inertia	J_1	J_2	J_3

End components of the waist, big arm, and forearm have total masses of m_1, m_2, and m_3 in kg, respectively. Centroids of the waist connecting rod, big arm, and forearm are d_1, d_2, and d_3 apart from the rotation center of the joint, measured in m. The gravity acceleration is vertically downward.

In a picking manipulator system, joint variables include the angle $q \in R^n$, the angular velocity $\dot{q} \in R^n$, and angular acceleration $\ddot{q} \in R^n$. The motor torque is $\tau \in R^n$. Then, we obtain

$$q = \begin{bmatrix} \theta_1 \\ \theta_2 \\ \theta_3 \end{bmatrix}, \quad \tau = \begin{bmatrix} \tau_1 \\ \tau_2 \\ \tau_3 \end{bmatrix}. \tag{1}$$

The kinetic energy of the lumbar joint can be obtained as

$$K_1 = \frac{1}{2} J_1 \dot{\theta}_1^{\,2}. \tag{2}$$

The kinetic energy of the big arm can be obtained as

$$K_2 = \frac{1}{2} J_2 \dot{\theta}_2^{\,2} + \frac{1}{2} m_{l2} \left(d_2 \sin\theta_2\right)^2 \dot{\theta}_1^{\,2} + \frac{1}{2} m_{l2} \left(d_2 \dot{\theta}_2\right)^2. \tag{3}$$

The total kinetic energy of the end element of the big arm can be obtained as

$$K_3 = \frac{1}{2}m_2\left(\dot{\theta}_1 l_2 \sin\theta_2\right)^2 + \frac{1}{2}m_2\left(\dot{\theta}_2 l_2\right)^2. \tag{4}$$

The kinetic energy of the forearm can be obtained as

$$\begin{aligned} K_4 = {} & \frac{1}{2}J_3\left(\dot{\theta}_2 + \dot{\theta}_3\right)^2 + \frac{1}{2}m_{l3}\left(\dot{\theta}_2 l_2 \sin\theta_3\right)^2 \\ & + \frac{1}{2}m_{l3}\left[\dot{\theta}_1 l_2 \sin\theta_2 + \dot{\theta}_1 d_3 \sin\left(\theta_2 + \theta_3\right)\right]^2 + \frac{1}{2}m_{l3}\left[\dot{\theta}_2 l_2 \cos\theta_3 + \left(\dot{\theta}_2 + \dot{\theta}_3\right)d_3\right]^2. \end{aligned} \tag{5}$$

The kinetic energy of the end element of the forearm can be obtained as

$$\begin{aligned} K_5 = {} & \frac{1}{2}m_3\left(\dot{\theta}_2 l_2\right)^2 + \frac{1}{2}m_3\left(\dot{\theta}_2 + \dot{\theta}_3\right)^2 {l_3}^2 + m_3 l_2 l_3 \left(\cos\theta_3\right)\dot{\theta}_2\left(\dot{\theta}_2 + \dot{\theta}_3\right) \\ & + \frac{1}{2}m_3\left(l_2 \sin\theta_2 + l_3 \sin\left(\theta_2 + \theta_3\right)\right)^2 {\dot{\theta}_1}^2. \end{aligned} \tag{6}$$

The potential energy of a picking manipulator can be obtained as

$$\begin{aligned} P = {} & m_{l1} g d_1 + m_1 g l_1 + m_{l2} g\left(l_1 + d_2 \cos\theta_2\right) + m_{l3} g\left(l_1 + l_2 \cos\theta_2 + d_3 \cos\left(\theta_2 + \theta_3\right)\right) \\ & + m_2 g\left(l_1 + l_2 \cos\theta_2\right) + m_3 g\left(l_1 + l_2 \cos\theta_2 + l_3 \cos\left(\theta_2 + \theta_3\right)\right). \end{aligned} \tag{7}$$

The Lagrange equation is derived from the above equations.

$$\begin{aligned} L = K - P = {} & \frac{1}{2}J_1 {\dot{\theta}_1}^2 + \frac{1}{2}J_2 {\dot{\theta}_2}^2 + \frac{1}{2}m_{l2}\left(d_2 \sin\theta_2\right)^2 {\dot{\theta}_1}^2 + \frac{1}{2}m_{l2}\left(d_2\dot{\theta}_2\right)^2 + \frac{1}{2}m_2\left(\dot{\theta}_1 l_2 \sin\theta_2\right)^2 + \frac{1}{2}m_2\left(\dot{\theta}_2 l_2\right)^2 \\ & + \frac{1}{2}J_3\left(\dot{\theta}_2 + \dot{\theta}_3\right)^2 + \frac{1}{2}m_{l3}\left[\dot{\theta}_1 l_2 \sin\theta_2 + \dot{\theta}_1 d_3 \sin\left(\theta_2 + \theta_3\right)\right]^2 + \frac{1}{2}m_{l3}\left(\dot{\theta}_2 l_2 \sin\theta_3\right)^2 + \frac{1}{2}m_3\left(\dot{\theta}_2 l_2\right)^2 + \frac{1}{2}m_{l3}\left[\dot{\theta}_2 l_2 \cos\theta_3 + \left(\dot{\theta}_2 + \dot{\theta}_3\right)d_3\right]^2 \\ & + \frac{1}{2}m_3\left(\dot{\theta}_2 + \dot{\theta}_3\right)^2 {l_3}^2 + m_3 l_2 l_3 \left(\cos\theta_3\right)\dot{\theta}_2\left(\dot{\theta}_2 + \dot{\theta}_3\right) + \frac{1}{2}m_3\left(l_2 \sin\theta_2 + l_3 \sin\left(\theta_2 + \theta_3\right)\right)^2 {\dot{\theta}_1}^2 \\ & - m_{l1} g d_1 - m_1 g l_1 - m_{l2} g\left(l_1 + d_2 \cos\theta_2\right) - m_2 g\left(l_1 + l_2 \cos\theta_2\right) \\ & - m_{l3} g\left(l_1 + l_2 \cos\theta_2 + d_3 \cos\left(\theta_2 + \theta_3\right)\right) - m_3 g\left(l_1 + l_2 \cos\theta_2 + l_3 \cos\left(\theta_2 + \theta_3\right)\right). \end{aligned} \tag{8}$$

Given the standard form of the Lagrange equation:

$$\frac{\mathrm{d}}{\mathrm{d}t}\frac{\partial L}{\partial \dot{q}} - \frac{\partial L}{\partial q} = \tau. \tag{9}$$

Based on equation (9), the dynamic equation of picking manipulators can be written in the following form:

$$M(q)\begin{bmatrix}\ddot{\theta}_1 \\ \ddot{\theta}_2 \\ \ddot{\theta}_3\end{bmatrix} + C(q,\dot{q})\begin{bmatrix}\dot{\theta}_1 \\ \dot{\theta}_2 \\ \dot{\theta}_3\end{bmatrix} + Q = \begin{bmatrix}\tau_1 \\ \tau_2 \\ \tau_3\end{bmatrix}, \tag{10}$$

where M, C, and Q are matrices of corresponding dimensions, respectively. In more detail,

$$
\begin{aligned}
M(q) &= \begin{bmatrix} M_{11} & M_{12} & M_{13} \\ M_{21} & M_{22} & M_{23} \\ M_{31} & M_{32} & M_{33} \end{bmatrix}, \\
M_{11} &= J_1 + m_{l2}\left(d_2 \sin\theta_2\right)^2 + m_2\left(l_2 \sin\theta_2\right)^2 + m_{l3}\left[l_2 \sin\theta_2 + d_3 \sin\left(\theta_2 + \theta_3\right)\right]^2 + m_3\left(l_2 \sin\theta_2 + l_3 \sin\left(\theta_2 + \theta_3\right)\right)^2, \\
M_{12} &= 0, M_{13} = 0, M_{21} = 0, \\
M_{22} &= J_2 + J_3 + m_{l2}{d_2}^2 + m_2{l_2}^2 + m_{l3}{l_2}^2 + 2m_{l3}d_3l_2\cos\theta_3 + m_{l3}{d_3}^2 + m_3{l_2}^2 + m_3{l_3}^2 + 2m_3l_2l_3\cos\theta_3, \\
M_{23} &= J_3 + m_{l3}d_3\left(l_2\cos\theta_3 + d_3\right) + m_3{l_3}^2 + m_3l_2l_3\cos\theta_3, M_{31} = 0, \\
M_{32} &= J_3 + m_3l_2l_3\left(\cos\theta_3\right) + m_{l3}d_3\left(l_2\cos\theta_3 + d_3\right) + m_3{l_3}^2, M_{33} = J_3 + m_{l3}{d_3}^2 + m_3{l_3}^2.
\end{aligned} \tag{11}
$$

In practical working processes, joint frictions and environment disturbances will always affect the mechanical picking arm. So, the practical dynamic model should be written as follows [35]:

$$
M(q)\ddot{q} + C(q,\dot{q})\dot{q} + F(\dot{q}) + G(q) + J^T(q)h + \tau_d = \tau, \tag{12}
$$

where $M(q) \in R^{n\times n}$ is the symmetric and positive definite inertia matrix and $C(q,\dot{q}) \in R^{n\times n}$ is the centrifugal and Coriolis term matrix. $F(\dot{q})$ includes $F_v(\dot{q})$ and F_d, with $F_v(\dot{q})$ being the viscous friction coefficient matrix and F_d being the dynamic friction term. $G(q) \in R^n$ represents the gravity vector. $J^T(q)$ denotes the geometric Jacobian matrix, so $J^T(q)h$ results in the generalized interaction forces. τ_d is the disturbance to the system.

The dynamics model of the picking system is written in the form of the state space, and an observer is designed to estimate its faults. The state vector of the system is expressed as $x = \begin{bmatrix} \varphi_1 \\ \varphi_2 \end{bmatrix} = \begin{bmatrix} q \\ \dot{q} \end{bmatrix} \in R^{2n}$. The system input is the motor torque $u = \tau \in R^n$, while its output is the angle of the manipulator $y = q \in R^n$.

According to equation (12) and the system state vector, we can obtain

$$
\begin{aligned}
\dot{\varphi}_2 = {} & M^{-1}(\varphi_1)\tau - M^{-1}(\varphi_1)J^T(\varphi_1)h - M^{-1}(\varphi_1)C(\varphi_1,\varphi_2)\varphi_2 \\
& - M^{-1}(\varphi_1)F(\varphi_2) - M^{-1}(\varphi_1)G(\varphi_1) - M^{-1}(\varphi_1)\tau_d.
\end{aligned} \tag{13}
$$

Then, the analytical model of the system can be described as follows:

$$
\begin{cases}
\dot{x}(t) = \begin{bmatrix} \dot{\varphi}_1(t) \\ \dot{\varphi}_2(t) \end{bmatrix} = \begin{bmatrix} 0_n & I_n \\ 0_n & 0_n \end{bmatrix}\begin{bmatrix} \varphi_1(t) \\ \varphi_2(t) \end{bmatrix} + \begin{bmatrix} 0_n \\ -M^{-1}(\varphi_1)\left(C(\varphi_1,\varphi_2)\varphi_2 + F(\varphi_2) + G(\varphi_1)\right) \end{bmatrix} \\
+ \begin{bmatrix} 0_n \\ -M^{-1}(\varphi_1)\tau_d \end{bmatrix} + \begin{bmatrix} 0_n \\ M^{-1}(\varphi_1) \end{bmatrix}\tau + \begin{bmatrix} 0_n \\ -M^{-1}(\varphi_1)J^T(\varphi_1) \end{bmatrix}h, \\
y = q = x_1 = \begin{bmatrix} I_n & 0_n \end{bmatrix}\begin{bmatrix} \varphi_1(t) \\ \varphi_2(t) \end{bmatrix},
\end{cases} \tag{14}
$$

where

$$
\begin{aligned}
A_0 &= \begin{bmatrix} 0_n & I_n \\ 0_n & 0_n \end{bmatrix}, \\
B_0 &= \begin{bmatrix} 0_n \\ M^{-1}(\varphi_1) \end{bmatrix}, \\
V_0(x) &= \begin{bmatrix} 0_n \\ -M^{-1}(\varphi_1)J^T(\varphi_1) \end{bmatrix}, \\
C_0 &= \begin{bmatrix} I_n & 0_n \end{bmatrix}, n_0(x) = \begin{bmatrix} 0_n \\ -M^{-1}(\varphi_1)\tau_d \end{bmatrix}, \\
F_0 f(x(t),u(t)) &= \begin{bmatrix} 0_n \\ -M^{-1}(\varphi_1)\left(C(\varphi_1,\varphi_2)\varphi_2 + F(\varphi_2) + G(\varphi_1)\right) \end{bmatrix}.
\end{aligned} \tag{15}
$$

3. State Estimation and Attack Reconstruction

From equation (14), the state-space equation of the picking robot CPS can be listed as follows:

$$\begin{cases} \dot{x}(t) = A_0 x(t) + B_0 u(t) + F_0 f_0(x(t), u(t)) + D_0 w(t), \\ y(t) = C_0 x(t) + H_0 v_s(t), \end{cases} \tag{16}$$

where $x(t) \in R^n$ is the state vector; $u(t) \in R^m$ is the system control input vector; $w(t) \in R^w$ denotes the system unknown input; $v_s(t) \in R^q$ denotes the sensor attacks; and $y(t) \in R^p$ represents the output. Initial states of the system $x(0) = x_0$. An errorless system should have $v_s(t) = 0$. In the attack detection, if the residual signal exceeds the threshold, the system can be identified with attacks. Coefficient matrices A_0, B_0, F_0, D_0, C_0, H_0 in the state equation have appropriate dimensions, and $A_0 \in R^{n\times n}$, $B_0 \in R^{n\times m}$, $D_0 \in R^{n\times w}$, $F_0 \in R^{n\times s}$, $C_0 \in R^{p\times n}$, $H_0 \in R^{p\times q}$ are given conditions, while $f\colon R^n \times R^m \longrightarrow R^s$ is a vector function. When the actuator failure is not considered, it can be assumed that C_0 is full rank in the row. F_0, D_0, and H_0 are matrices with full column rank, and their dimensions satisfy the following conditions:

$$p \geq w + q. \tag{17}$$

Assumption 1. The nonlinear function satisfies the Lipschitz condition, and then we can have

$$\left\| f_0(x_1(t), u(t)) - f_0(x_2(t), u(t)) \right\| \leq \delta \left\| x_1 - x_2 \right\|. \tag{18}$$

Remark 1. The Lipschitz assumption given in this paper is reasonable, and similar assumptions are made as in [28, 30]. The system features a noteworthy nonlinearity. In the following proposed attack construction method, nonlinear parts are all treated under the Lipschitz condition. A more accurate system model needs to be established for considering the nonlinear part of the system that violates the Lipschitz condition.

When the actuator attacks are not considered, the system can be affected by unknown inputs and $y(t)$ changes, which means the sensor attacks and noise exist simultaneously in the system [20]. Assuming $d(t)$ is a noise signal, $\text{rank}(G_d) = l$, equation (14) can be transformed into

$$\begin{cases} \dot{x}(t) = A_0 x(t) + B_0 u(t) + F_0 f_0(x(t), u(t)) + D_0 w(t) + D_d d(t), \\ y(t) = C_0 x(t) + H_0 v_s(t) + G_d d(t). \end{cases} \tag{19}$$

Let

$$\begin{aligned} G_d &= \begin{bmatrix} I_l & 0 \\ 0 & 0 \end{bmatrix}, \\ d(t) &= \begin{bmatrix} d_1(t) \\ d_2(t) \end{bmatrix}, \\ y(t) &= \begin{bmatrix} y_1(t) \\ y_2(t) \end{bmatrix}, \\ D_d &= \begin{bmatrix} D_{d1} & D_{d2} \end{bmatrix}, \\ C_0 &= \begin{bmatrix} C_1 \\ C_2 \end{bmatrix}. \end{aligned} \tag{20}$$

Then, we can obtain results as follows:

$$\begin{aligned} &\begin{cases} y_1(t) = C_1 x(t) + H_1 v_s(t) + d_1(t), \\ y_2(t) = C_2 x(t) + H_2 v_s(t), \end{cases} \\ \dot{x}(t) &= \left(A_0 - D_{d_1} C_1\right) x(t) + B_0 u(t) + F_0 f_0(x(t), u(t)) + D_0 w(t) \\ &\quad + D_{d_1} y_1(t) - D_{d_1} H_1 v_s(t) + D_{d_2} d_2(t). \end{aligned} \tag{21}$$

3.1. Augmented Transformation of System State. In this section, we use the augmented transformation method to estimate states of the system without considering actuator attacks. The augmented state vector of the system is shown as follows:

$$\overline{x} = \begin{bmatrix} x(t) \\ v_s(t) \end{bmatrix}. \tag{22}$$

Let

$$E = \begin{bmatrix} I & 0 \\ 0 & 0 \end{bmatrix},$$

$$B = \begin{bmatrix} B_0 \\ 0 \end{bmatrix},$$
$$C = \begin{bmatrix} C_0 & H_0 \end{bmatrix},$$
$$D = \begin{bmatrix} D_0 \\ 0 \end{bmatrix}. \tag{23}$$

Then, equation (16) can be transformed into

$$\begin{cases} \begin{bmatrix} I & 0 \\ 0 & 0 \end{bmatrix} \begin{bmatrix} \dot{x}(t) \\ \dot{v}_s(t) \end{bmatrix} = \begin{bmatrix} A_0 & 0 \\ 0 & 0 \end{bmatrix} \begin{bmatrix} x(t) \\ v_s(t) \end{bmatrix} + \mathrm{Bu}(t) + Ff\left(\left(\begin{bmatrix} I & 0 \\ 0 & 0 \end{bmatrix} \begin{bmatrix} x(t) \\ v_s(t) \end{bmatrix}\right), u(t)\right) + Dw(t), \\ y(t) = \begin{bmatrix} C_0 & H_0 \end{bmatrix} \begin{bmatrix} x(t) \\ v_s(t) \end{bmatrix}. \end{cases} \tag{24}$$

Therefore, the system state equation can be augmented to be

$$\left\{ E\dot{\overline{x}}(t) = A\overline{x}(t) + Bu(t) + Ff\left(E\overline{x}(t), u(t)\right) + Dw(t),\ y(t) = C\overline{x}(t). \right. \tag{25}$$

Lemma 1. *There are matrices* $T \in R^{(n+q)\times(n+q)}$ *and* $H \in R^{(n+q)\times p}$ *such that*

$$\begin{bmatrix} T & H \end{bmatrix}_{(n+q)\times(n+p+q)} \begin{bmatrix} E_{(n+q)\times(n+q)} \\ C_{p\times(n+q)} \end{bmatrix} = I_{n+q}, \tag{26}$$

satisfying

$$TE + HC = I_{n+q}. \tag{27}$$

Proof of Lemma 1. Given $C \in R^{p\times(n+q)}$, $E \in R^{(n+q)\times(n+q)}$, and H_0 is a full column rank matrix, $\Omega = \begin{bmatrix} E \\ C \end{bmatrix} = \begin{bmatrix} I & 0 \\ C_0 & H_0 \end{bmatrix}$ is a matrix with full column rank. From the equation $\begin{bmatrix} T & H \end{bmatrix}\Omega = I_{n+q}$, the following equation can be obtained:

$\begin{bmatrix} T & H \end{bmatrix} = \Omega^{+} - U\left(I_{n+q+p} - \Omega\Omega^{+}\right)$, where $U \in R^{(n+q)\times(n+q+p)}$ is an arbitrary matrix, so we can obtain the following results:

$$\begin{aligned} T &= \left[\Omega^{+} - U\left(I_{n+q+p} - \Omega\Omega^{+}\right)\right] \begin{bmatrix} I_{n+q} \\ 0_{p\times(n+q)} \end{bmatrix}, \\ H &= \left[\Omega^{+} - U\left(I_{n+q+p} - \Omega\Omega^{+}\right)\right] \begin{bmatrix} 0_{(n+q)\times p} \\ I_p \end{bmatrix}. \end{aligned} \tag{28}$$

□

3.2. H_∞ Unknown Input Observer Design. The unknown input observer is designed based on the system state shown by equation (25). The observer is given as follows:

$$\left\{ \dot{\varepsilon}(t) = P\varepsilon(t) + Ny(t) + Ju(t) + TFf\left(E\widehat{\overline{x}}(t), u(t)\right), \widehat{\overline{x}}(t) = \varepsilon(t) + Hy(t), \widehat{y}(t) = C\widehat{\overline{x}}(t). \right. \tag{29}$$

In equation (29), $\varepsilon(t) \in R^{n+q}$ is the observer state, $\widehat{\overline{x}}(t) \in R^{n+q}$ is the estimation of the augmented state vector, and $\widehat{y}(t)$ is the estimation of $y(t)$. The coefficient matrices P, N, J, T, H, F, C have appropriate dimensions, and these matrices need to be known. In this way, system (29) serves as an observer of system (25) in a certain sense. We can define the observer error as $e(t) = \widehat{\overline{x}}(t) - \overline{x}(t)$. For the case of $w(t) = 0$, the error approaches zero, while for $w(t) \neq 0$, we can solve

$$\mathrm{minsup}_{\omega\in L_2-\{0\}} \frac{\|e\|_{L_2}}{\|\omega\|_{L_2}}. \tag{30}$$

From equations (27) and (29),

$$e(t) = \widehat{\overline{x}}(t) - \overline{x}(t) = \varepsilon(t) - (I - HC)\overline{x}(t) = \varepsilon(t) - TE\overline{x}(t). \tag{31}$$

We can have

$$\begin{aligned} \dot{e}(t) = \dot{\varepsilon}(t) - TE\dot{\overline{x}}(t) = P\varepsilon(t) + Ny(t) + Ju(t) + TFf(E\widehat{\overline{x}}(t), u(t)) \\ -T(A\overline{x}(t) + Bu(t) + Ff(E\overline{x}(t), u(t)) + Dw(t)) = \\ Pe(t) + (\mathrm{PTE} + NC - TA)\overline{x}(t) + (J - TB)u(t) + TF\Delta f - T\ Dw(t). \end{aligned} \tag{32}$$

In equation (32), we assume that the coefficient matrices $P \in R^{(n+q)\times(n+q)}$ and $N \in R^{(n+q)\times p}$ satisfy the following conditions:

$$\begin{cases} \mathrm{PTE} - TA + NC = 0, \\ J - TB = 0. \end{cases} \tag{33}$$

Then, equation (32) turns out to be

$$\dot{e}(t) = Pe(t) + TF\Delta f - TDw(t). \tag{34}$$

Substituting (27) into (33), we can obtain

$$P = TA - (N - PH)C. \tag{35}$$

When the arbitrary matrix K satisfies $K = N - PH$, we can determine and from equation (33):

$$P = TA - KC, \tag{36}$$

$$N = PH + K. \tag{37}$$

Lemma 2. *For the case of $w(t) = 0$, there are two positive definite matrices W and X_0, equation (34) can be asymptotically stable if the following conditions are satisfied.*

$$\begin{aligned} W < I, \\ \begin{bmatrix} P^T X_0 + X_0 P + \delta^2 E^T E & X_0(TF) \\ (TF)^T X_0 & -W \end{bmatrix} < 0. \end{aligned} \tag{38}$$

Proof of Lemma 2. Consider the Lyapunov function:

$$V(t) = e^T(t) X_0 e(t), \tag{39}$$

where X_0 is a positive definite and real symmetric matrix. Then, we can have

$$\begin{aligned} \dot{V}(t) &= \dot{e}^T(t) X_0 e(t) + e^T(t) X_0 \dot{e}(t) \\ &= (Pe(t) + (TF)\Delta f)^T X_0 e(t) + e^T(t) X_0 (Pe(t) + (TF)\Delta f) \\ &= e^T(t)\left(P^T X_0 + X_0 P\right)e(t) + \Delta f^T (TF)^T X_0 e(t) + e^T(t) X_0 (TF)\Delta f. \end{aligned} \tag{40}$$

If the dynamic error system is stable, the following conditions must be satisfied:

$$\dot{V}(t) \le e^T(t)\left(P^T X_0 + X_0 P\right)e(t) + \Delta f^T (TF)^T X_0 e(t) + e^T(t) X_0 (TF)\Delta f + \Delta f^T \Delta f - \Delta f^T W \Delta f. \tag{41}$$

According to $\Delta f = f(\widehat{\overline{x}}(t), u(t)) - f(\overline{x}(t), u(t))$ and the Lipschitz condition, there are constants such that

$$\|f(E\widehat{\overline{x}}(t), u(t)) - f(E\overline{x}(t), u(t))\| \le \delta \|E\widehat{\overline{x}} - E\overline{x}\|. \tag{42}$$

Therefore,

$$\Delta f^T \Delta f \le \left\|\Delta f^T\right\| \|\Delta f\| \le \delta^2 e^T(t) E^T E e(t). \tag{43}$$

Equation (41) is equivalent to the following form:

$$\begin{aligned} \dot{V}(t) &\le e^T(t)\left(P^T X_0 + X_0 P\right)e(t) + \Delta f^T (TF)^T X_0 e(t) \\ &\quad + e^T(t) X_0 (TF)\Delta f + \Delta f^T \Delta f - \Delta f^T W \Delta f \\ &= \begin{bmatrix} e^T(t) & \Delta f^T \end{bmatrix} Q_0 \begin{bmatrix} e(t) \\ \Delta f \end{bmatrix}, \\ Q_0 \text{ is} &\begin{bmatrix} P^T X_0 + X_0 P + \delta^2 E^T E & X_0(TF) \\ (TF)^T X_0 & -W \end{bmatrix}. \end{aligned} \tag{44}$$

The asymptotically stable condition of the error system is that $\dot{V}(t)$ is a negative definite function, so $Q < 0$, and it can be proved.

The conditions can be determined from the error dynamics equation and under the satisfied assumptions to make the system stable. For the observer, we can determine H_∞ performance indicator $\gamma > 0$, constant $\lambda \geq 0$. Let

$$\Phi = \begin{bmatrix} (XTA)^T - (MC)^T + XTA - MC + I + \lambda\delta^2 I & X(TF) & -X(TD) \\ (TF)^T X & -\lambda I & 0 \\ -(TD)^T X & 0 & -\gamma^2 I \end{bmatrix}. \tag{45}$$

Theorem 1. *Assume the following LMI:*

$$\Phi < 0. \tag{46}$$

For positive definite matrices $X \in R^{(n+q)\times(n+q)}$ and $M \in R^{(n+q)\times p}$, (49) has a solvable solution. Let $K = X^{-1}M$. Then, (29) is a meaningful observer.

Proof of Theorem 1. X is a positive definite matrix. Consider the Lyapunov function as follows:

$$V(t) = e^T(t)Xe(t). \tag{47}$$

From equation (34), it can be known that

$$\dot{V}(t) = \dot{e}^T(t)Xe(t) + e^T(t)X\dot{e}(t) = e^T(t)\left(P^T X + XP\right)e(t) + \Delta f^T (TF)^T Xe(t) - w^T(t)(TD)^T Xe(t) + e^T(t)X(TF)\Delta f - e^T(t)XTDw(t). \tag{48}$$

Therefore,

$$\dot{V}(t) \leq e^T(t)\left(P^T X + XP\right)e(t) + \Delta f^T (TF)^T Xe(t) - w^T(t)(TD)^T Xe(t) + e^T(t)\mathrm{XTF}\Delta f - e^T(t)\mathrm{XTD}w(t) + \lambda\delta^2 e^T e - \lambda\Delta f^T \Delta f, \tag{49}$$

and

$$\begin{aligned} &\dot{V}(t) + e^T e - \gamma^2 w^T(t)w(t) \\ &\leq e^T(t)\left(P^T X + XP\right)e(t) + \Delta f^T (TF)^T Xe(t) - w^T(t)(TD)^T Xe(t) + e^T(t)\mathrm{XTF}\Delta f \\ &\quad - e^T(t)\mathrm{XTD}w(t) + \lambda\delta^2 e^T e - \lambda\Delta f^T\Delta f + e^T e - \gamma^2 w^T(t)w(t) \\ &= \begin{bmatrix} e^T & \Delta f^T & w^T \end{bmatrix}\Phi_1 \begin{bmatrix} e \\ \Delta f \\ w \end{bmatrix}, \end{aligned} \tag{50}$$

in which

$$\Phi_1 = \begin{bmatrix} P^T X + XP + I + \lambda\delta^2 I & X(TF) & -X(TD) \\ (TF)^T X & -\lambda I & 0 \\ -(TD)^T X & 0 & -\gamma^2 I \end{bmatrix} < 0. \tag{51}$$

According to (36) and (37) and $K = X^{-1}M$, a result can be obtained by the transformation:

$$\Phi_{11} = (XTA)^T - (MC)^T + XTA - MC + I + \lambda\delta^2 I. \tag{52}$$

Considering equation (50), if $\Phi_1 < 0$, then

$$\dot{V}(t) + e^T e - \gamma^2 w^T(t)w(t) \leq \begin{bmatrix} e^T & \Delta f^T & w^T \end{bmatrix}\Phi_1 \begin{bmatrix} e \\ \Delta f \\ w \end{bmatrix} < 0. \tag{53}$$

Therefore,

$$\int_0^\infty \dot{V}(t)dt < \int_0^\infty \gamma^2 w^T(t)w(t)dt - \int_0^\infty e^T(t)e(t)dt. \quad (54)$$

Equation (54) is equivalent to the following form:

$$V(\infty) - V(0) < \gamma^2 \|w(t)\|_2^2 - \|e(t)\|_2^2. \quad (55)$$

Under the prerequisite that the initial condition is zero, we can obtain

$$\begin{aligned} &\gamma^2 \|w(t)\|_2^2 - \|e(t)\|_2^2 > 0, \\ &\gamma^2 \|w(t)\|_2^2 > \|e(t)\|_2^2. \end{aligned} \quad (56)$$

So, the theorem is proved. □

4. Simulation Verification

In this section, numerical simulations are carried out to verify the effectiveness of the proposed method. The base material is steel, and the waist, arm, and forearm material are all made of aluminum alloy 6061. The model parameters of the manipulator are listed in Table 2.

Coefficient matrices are calculated as follows:

$$E = \begin{bmatrix} 1&0&0&0&0&0&0 \\ 0&1&0&0&0&0&0 \\ 0&0&1&0&0&0&0 \\ 0&0&0&1&0&0&0 \\ 0&0&0&0&1&0&0 \\ 0&0&0&0&0&1&0 \\ 0&0&0&0&0&0&0 \end{bmatrix}, A = \begin{bmatrix} 0&0&0&1&0&0&0 \\ 0&0&0&0&1&0&0 \\ 0&0&0&0&0&1&0 \\ 0&0&0&0&0&0&0 \\ 0&0&0&0&0&0&0 \\ 0&0&0&0&0&0&0 \\ 0&0&0&0&0&0&0 \end{bmatrix}, C = \begin{bmatrix} 1&0&0&0&0&0&1 \\ 0&1&0&0&0&0&1 \\ 0&0&1&0&0&0&1.7 \\ 0&0&0&1&0&0&1.7 \end{bmatrix},$$
$$B = \begin{bmatrix} 0&0&0 \\ 0&0&0 \\ 0&0&0 \\ 0.1339&0&0 \\ 0&0.1179&-0.2228 \\ 0&-0.2209&0.9467 \\ 0&0&0 \end{bmatrix}, D = \begin{bmatrix} 0.1 \\ 0.1 \\ 0.1 \\ 0.1 \\ 0.1 \\ 0.1 \\ 0 \end{bmatrix}, F = \begin{bmatrix} 1 \\ 1 \\ 1 \\ 1 \\ 1 \\ 1 \\ 0 \end{bmatrix}. \quad (57)$$

From equations (43) and (44), we can obtain results as follows:

$$T = \begin{bmatrix} 8.5177&-9.9256&-10.9620&12.3784&0&0&0 \\ -47.1612&45.7533&34.9002&-33.4838&0&0&0 \\ -13.9555&11.5620&-22.1311&24.5390&0&0&0 \\ 29.9152&-32.3087&20.4127&-18.0048&0&0&0 \\ -0.3915&-2.0019&-11.0319&12.4398&1&0&0 \\ -13.4733&11.0466&-2.0668&3.4943&0&1&0 \\ 1.3498&0.0581&-1.9020&0.4855&0&0&0 \end{bmatrix},$$
$$H = \begin{bmatrix} -7.5177&9.9256&10.9620&-12.3784 \\ 47.1612&-44.7533&-34.9002&33.4838 \\ 13.9555&-11.5620&23.1311&-24.5390 \\ -29.9152&32.3087&-20.4127&19.0048 \\ 0.3915&2.0019&11.0319&-12.4398 \\ 13.4733&-11.0466&2.0668&-3.4943 \\ -1.3498&-0.0581&1.9020&-0.4855 \end{bmatrix}, \quad (58)$$

where $w(t)$ is the unknown input, and the nonlinear term is set to be

$$f_0(x(t), u(t)) = 80\cos(5t) + 0.1. \quad (59)$$

The first sensor attack takes the following abrupt constant form:

$$v_1 = \begin{cases} 0, & 0 \le t < 3, \\ 30, & 3 \le t < 5, \\ 0, & 5 \le t < 10. \end{cases} \quad (60)$$

The second sensor attack takes the following ramp function form:

$$v_2 = \begin{cases} 0, & 0 \le t < 2, \\ 30(t-1), & 2 \le t < 6, \\ 30, & 6 \le t < 10. \end{cases} \quad (61)$$

The third sensor attack takes the following trigonometric function form:

$$v_3 = \begin{cases} 0, & 0 \le t < 2, \\ 80\cos(5t-1) + 30\sin 5t, & 2 \le t < 6, \\ 0, & 6 \le t < 10. \end{cases} \quad (62)$$

The feasible solution of LMI equation (49) can be obtained by simulation software, and $\lambda = 3$. The Mincx function is used to find the minimum value of γ. Therefore,

Table 2: Model parameters of the robot.

Parameter	Description	Value
l_1	Length of waist joint	0.05 m
l_2	Length of big arm	0.65 m
l_3	Length of forearm	0.42 m
m_{l1}	Mass of waist	22.6 kg
m_{l2}	Mass of big arm	7.9 kg
m_{l3}	Mass of forearm	9.8 kg
m_1	Mass of waist joint end parts	5.57 kg
m_2	Mass of shoulder joint end parts	6.38 kg
m_3	Masses of elbow joint end parts	4.29 kg
d_1	Distance from waist joint rotation center to the centroid of waist connecting rod	0.12 m
d_2	Distance from shoulder joint rotation center to the centroid of big arm	0.25 m
d_3	Distance from elbow joint rotation center to the centroid of forearm	0.33 m
J_1	Inertia of waist connecting rod	0.26 kg·m^2
J_2	Inertia of big arm	0.77 kg·m^2
J_3	Inertia of forearm	0.06 kg·m^2

according to $K = X^{-1}M$, coefficient matrices can be obtained as follows:

$$K = \begin{bmatrix} 2.0269 & -11.1166 & 121.0997 & 59.8433 \\ 11.3664 & 2.4206 & 83.8526 & 41.2676 \\ -121.3742 & -83.4578 & 1.8400 & -113.8647 \\ -51.2350 & -87.6688 & 100.0123 & 32.3760 \\ -10.1048 & 46.2433 & 11.2063 & -32.4351 \\ -10.9741 & 34.9234 & -22.1543 & 6.9489 \\ -298.4800 & -226.8516 & 395.3608 & -85.0850 \end{bmatrix}. \quad (63)$$

Simulation results are shown in Figures 3–8, in which Figures 3–5 demonstrate some system state estimations exclusive of actuator attacks. In these figures, solid lines represent actual system states, while dotted lines represent their estimated values. Figures 6–8 show distributions of the actual and estimated values of sensor attacks. It can be seen from Figures 3–5 that the estimations of system states gradually approximate their actual values, indicating good performances of the designed observer. In the simulation, the dimension of the system variable is six, and the dimension of the augmented system is seven. The data of the seventh dimension refer to the attack signal of the sensor. Figure 3 shows the actual signal and estimation signal of the rotation angle variable of one joint, and Figures 4 and 5 show the actual signal and estimation signal of the angular velocity of two joints. Figures 6–8 show the reconstruction of three kinds of sensor attack signals. In Figure 6, the attack signal is an abrupt constant form, in Figure 7, the attack signal is a ramp function form, and in Figure 8, the attack signal is the form of trigonometric function. These three kinds of attack signals are used to better test the reconstruction performance of the system for sensor attack signals. Significantly, it can be seen from Figures 6–8 that the designed observer can effectively suppress the influence of system nonlinearities and external disturbances over attack detection, indicative of a good performance in sensor attack detection.

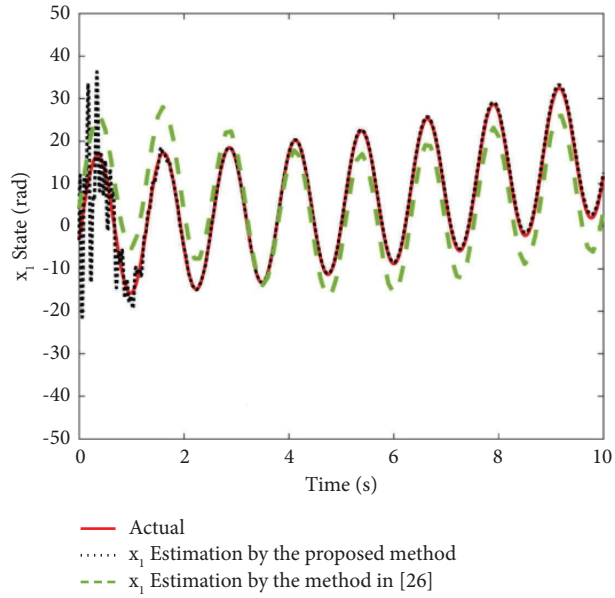

Figure 3: State and its estimation (x_1).

5. Discussion

Fruit and vegetable picking robot CPS can alleviate the insufficiency of agricultural labor and appreciably improve productivity. As a typical ACPS, it would be up against complicated and changeable agricultural production environments, whereupon how to effectively handle the attacks on sensors for the picking success has become a crux in developing agricultural picking robot cyber-physical system. In contrast to a less requirement for precision in practical applications of the picking robots, high reliability is however quite needed. Therefore, the development of novel picking robot CPS requires their attack reconstruction systems to have excellent robustness and real-time performance. It is exactly the above consideration that makes the present study have practical significance.

In the context of agricultural production, this paper involves the widely used picking robot CPS, for which the sensor attacks are considered on the basis of the dynamic

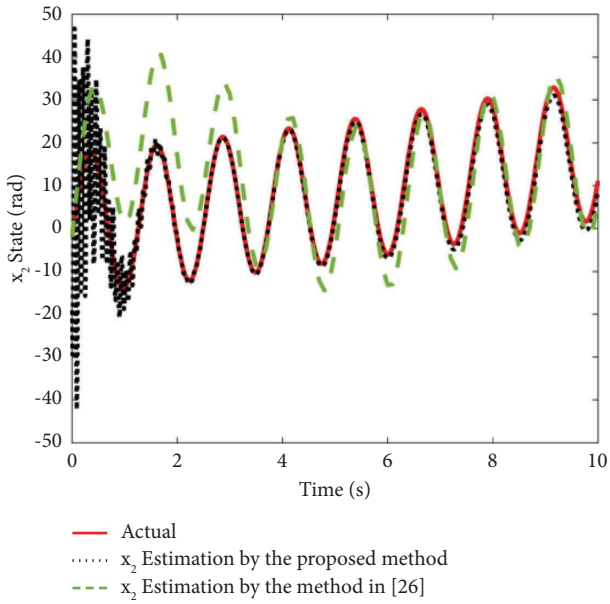

Figure 4: State and its estimation (x_2).

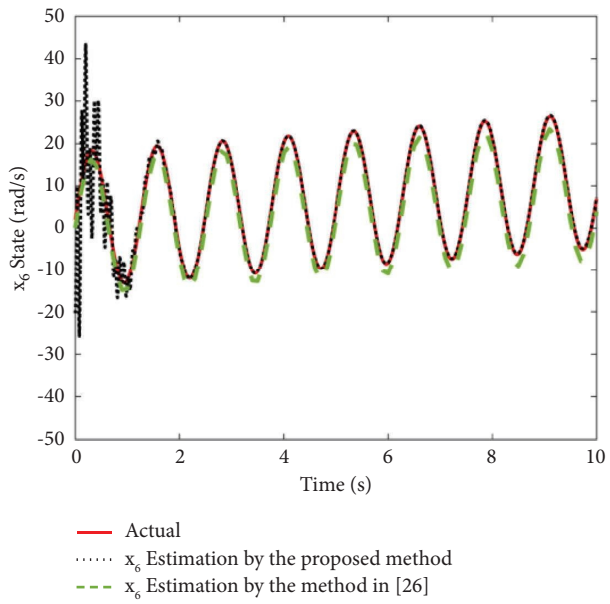

Figure 5: State and its estimation (x_6).

model. Such a model contributes to the formulation of state-space equations, which is a mature method at present. Besides, this paper directly embeds the CAD model data of the three-joint robot in simulative verification, which can thus provide a novel method on sensor attack detection for picking robot cyber-physical system, so as to facilitate the development of fault diagnosis systems for agricultural gathering equipment.

Simulation results demonstrate that estimated values approach real states very well, suggesting the feasibility of the proposed method. In particular, the formulation of state equations defines a 6-D state vector, representing rotation angles and angular velocities for the three joints.

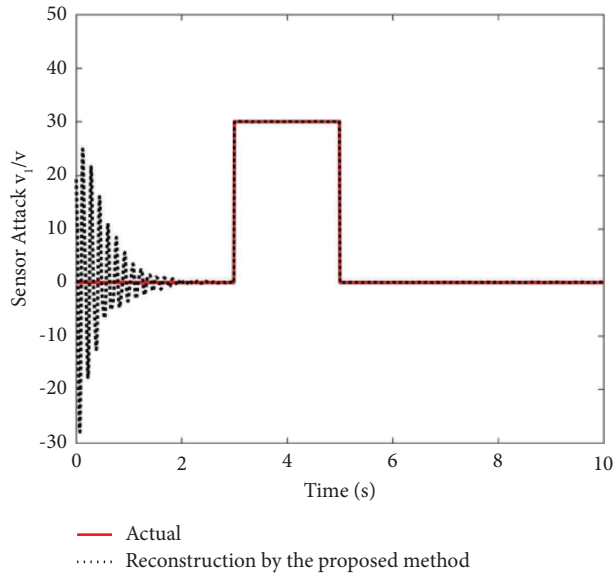

Figure 6: Attack reconstruction of the first form.

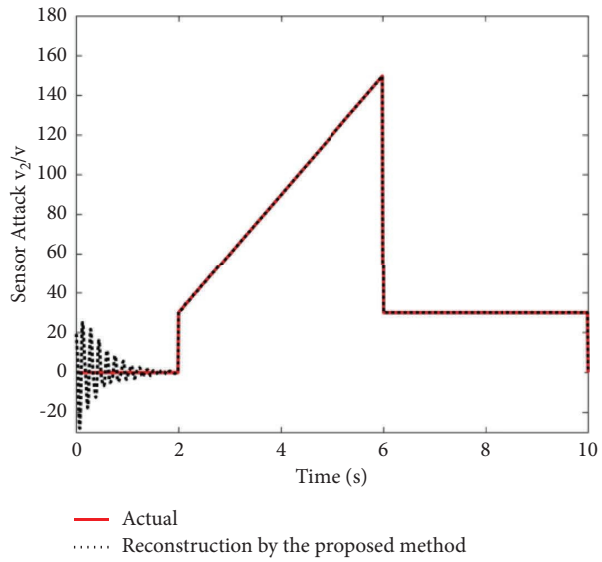

Figure 7: Attack reconstruction of the second form.

The displacement and velocity of joints can directly characterize the picking state of robots, so the proposed method conforms to realistic scenes and thus has practical applications.

Nevertheless, the system features a noteworthy nonlinearity, which increases the difficulty in modeling such a nonlinear system [38]. In the proposed attack construction method, nonlinear parts are all treated under the Lipschitz qualification. In the future work, the nonlinearity of the system will be considered in more depth, involving those violating the Lipschitz condition [39]. Further, the mechanical arm system will be fully considered in terms of other local nonlinearities, joint frictions, the coupling of rigidity and flexibility in connecting rods, etc., so as to establish a more practical attack model for the system and propose a more effective attack construction method.

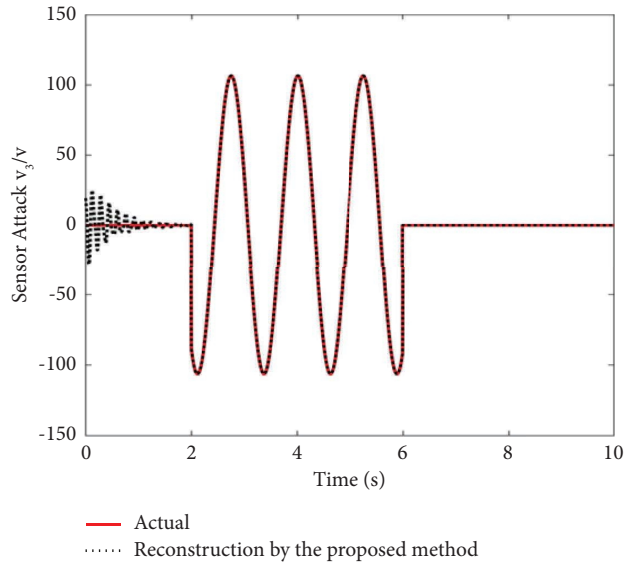

Figure 8: Attack reconstruction of the third form.

6. Conclusions

In this paper, an unknown input observer-based method is proposed to address estimations of system states and sensor attack reconstruction for fruit and vegetable picking robot CPS. Based on the dynamic model of the system, the state-space model following the actual working condition is established, with the system nonlinearity and external disturbance taken into account.

Using the generalized system theory, sensor attacks of the picking robot cyber-physical system are treated as parts of system state variables, thus in favour of sensor attack estimations. Simulation results have shown the effectiveness of the proposed method and demonstrated that the designed observer performs well in sensor attack reconstruction. Future works will be conducted to further test the practical performance of the proposed method using actual picking robot CPS. More to the point, the future work will focus on the operation state of the cyber-physical system as well as the mechanism of their attack occurrences, so as to underpin the design of complicated picking equipment. These contents need to be studied in the future.

Data Availability

The data that support the findings of the study are available from the corresponding author upon request.

Conflicts of Interest

The authors declare that there are no conflicts of interest regarding the publication of this paper.

Acknowledgments

This research was funded by the National Natural Science Foundation of China (61703296), the Special Project for Tackling Key Common Technologies of Agricultural High-Quality Development in Hebei Province (21327214D), and the Food Processing Discipline Group of Hebei Agricultural University.

References

[1] R. Pal and V. Prasanna, "The STREAM mechanism to improve CPS security the case of the smart grid," *IEEE Transactions on Computer-Aided Design of Integrated Circuits and Systems*, vol. 36, no. 4, pp. 537–550, 2017.

[2] Y. Xie, G. Zeng, R. Kurachi, F. Xiao, and H. Takada, "Optimizing extensibility of CAN FD for automotive cyber-physical systems," *IEEE Transactions on Intelligent Transportation Systems*, vol. 22, no. 12, pp. 7875–7886, 2021.

[3] A. Bagozi, D. Bianchini, and V. De Antonellis, "Multi-level and relevance-based parallel clustering of massive data streams in smart manufacturing," *Information Sciences*, vol. 577, no. 9, pp. 805–823, 2021.

[4] M. Naghnaeian, N. H. Hirzallah, and P. G. Voulgaris, "Security via multirate control in cyber-physical systems," *Systems & Control Letters*, vol. 124, pp. 12–18, 2019.

[5] A. K. Sutrala, M. S. Obaidat, S. Saha, A. K. Das, M. Alazab, and Y. Park, "Authenticated Key agreement scheme with user anonymity and untraceability for 5G-enabled softwarized industrial cyber-physical systems," *IEEE Transactions on Intelligent Transportation Systems*, vol. 23, no. 3, pp. 2316–2330, 2022.

[6] P. O. Dusadeerungsikul, S. Y. Nof, A. Bechar, and Y. Tao, "Collaborative control protocol for agricultural cyber-physical system," *Procedia Manufacturing*, vol. 39, pp. 235–242, 2019.

[7] A. Selmani, H. Oubehar, M. Outanoute et al., "Agricultural cyber-physical system enabled for remote management of solar-powered precision irrigation," *Biosystems Engineering*, vol. 177, pp. 18–30, 2019.

[8] A. Roshanianfard, T. Kamata, and N. Noguchi, "Performance evaluation of harvesting robot for heavy-weight crops," *IFAC-PapersOnLine*, vol. 51, no. 17, pp. 332–338, 2018.

[9] J. Michniewicz and G. Reinhart, "Cyber-Physical-Robotics – modelling of modular robot cells for automated planning and execution of assembly tasks," *Mechatronics*, vol. 34, pp. 170–180, 2016.

[10] S.-H. Choi, I.-B. Jeong, J.-H. Kim, and J. J. Lee, "Context generator and behavior translator in a multilayer architecture for a modular development process of cyber-physical robot systems," *IEEE Transactions on Industrial Electronics*, vol. 61, no. 2, pp. 882–892, 2014.

[11] J. Nikander, O. Manninen, and M. Laajalahti, "Requirements for cybersecurity in agricultural communication networks," *Computers and Electronics in Agriculture*, vol. 179, Article ID 105776, 2020.

[12] H. Jain, M. Kumar, and A. M. Joshi, "Intelligent energy cyber physical systems (iECPS) for reliable smart grid against energy theft and false data injection," *Electrical Engineering*, vol. 104, no. 1, pp. 331–346, 2021.

[13] M. Sayad Haghighi, F. Farivar, A. Jolfaei, and M. H. Tadayon, "Intelligent robust control for cyber-physical systems of rotary gantry type under denial of service attack," *The Journal of Supercomputing*, vol. 76, no. 4, pp. 3063–3085, 2019.

[14] M. S. Mahmoud, M. M. Hamdan, and U. A. Baroudi, "Modeling and control of Cyber-Physical Systems subject to cyber attacks: a survey of recent advances and challenges," *Neurocomputing*, vol. 338, pp. 101–115, 2019.

[15] G. Franzè, F. Tedesco, and D. Famularo, "Model predictive control for constrained networked systems subject to data losses," *Automatica*, vol. 54, pp. 272–278, 2015.

[16] J. G. Lee, J. Kim, and H. Shim, "Fully distributed resilient state estimation based on distributed median solver," *IEEE Transactions on Automatic Control*, vol. 65, no. 9, pp. 3935–3942, 2020.

[17] A. Lu and G. Yang, "Event-triggered secure observer-based control for cyber-physical systems under adversarial attacks," *Information Sciences*, vol. 420, pp. 96–109, 2017.

[18] Z. Zhao, Y. Huang, Z. Zhen, and Y. Li, "Data-driven false data-injection attack design and detection in cyber-physical systems," *IEEE Transactions on Cybernetics*, vol. 51, no. 12, pp. 6179–6187, 2021.

[19] Z. Hong, C. Yang, and L. Yu, " A system residuals-based fingerprinting for attack detection in industrial cyber-physical systems," *IEEE Transactions on Industrial Electronics*, vol. 68, no. 11, Article ID 3029488, 2021.

[20] W. Lucia, K. Gheitasi, and M. Ghaderi, "Setpoint Attack detection in cyber-physical systems," *IEEE Transactions on Automatic Control*, vol. 66, no. 5, pp. 2332–2338, 2021.

[21] Y. Shoukry, P. Nuzzo, A. Puggelli, A. Sangiovanni-Vincentelli, S. A. Seshia, and P. Tabuada, "Secure state estimation for cyber-physical systems under sensor attacks:A satisfiability modulo theory approach," *IEEE Transactions on Automatic Control*, vol. 62, no. 10, pp. 4917–4932, 2017.

[22] A. Y. Lu and A Yang, "Input-to-State stabilizing control for cyber-physical systems with multiple transmission channels under denial of service," *IEEE Transactions on Automatic Control*, vol. 63, no. 6, pp. 1813–1820, 2018.

[23] X. Huang and J. Dong, "Reliable control policy of cyber-physical systems against a class of frequency-constrained sensor and actuator attacks," *IEEE Transactions on Cybernetics*, vol. 48, no. 12, pp. 3432–3439, 2018.

[24] M. Farza, M. M'Saad, T. Ménard, A. Ltaief, and T. Maatoug, "Adaptive observer design for a class of nonlinear systems. Application to speed sensorless induction motor," *Automatica*, vol. 90, pp. 239–247, 2018.

[25] M. D. Tran and H. J. Kang, "Nonsingular terminal sliding mode control of uncertain second-order nonlinear systems," *Mathematical Problems in Engineering*, vol. 2015, pp. 1–8, Article ID 181737, 2015.

[26] A. Zemouche and M. Boutayeb, "On LMI conditions to design observers for Lipschitz nonlinear systems," *Automatica*, vol. 49, no. 2, pp. 585–591, 2013.

[27] S. Guo and F. Zhu, "Reduced-order observer design for discrete-time descriptor systems with unknown inputs: an linear matrix inequality approach," *Journal of Dynamic Systems, Measurement, and Control*, vol. 1378 pages, Article ID 084503, 2015.

[28] N. Gasmi, M. Boutayeb, A. Thabet, and M. Aoun, "Enhanced LMI conditions for observer-based H_∞ stabilization of Lipschitz discrete-time systems," *European Journal of Control*, vol. 44, pp. 80–89, 2018.

[29] K. Lee, J. Lee, J. Back, and Y. I. Lee, "A robust emulation of mechanical loads using a disturbance-observer," *Energies*, vol. 12, no. 12, Article ID 2236, 2019.

[30] M. Darouach, L. Boutat-Baddas, and M. Zerrougui, "H_∞ Observers design for a class of nonlinear singular systems," *Automatica*, vol. 47, pp. 2517–2525, 2011.

[31] A. Y. Lu and G. H. Yang, "Secure switched observers for cyber-physical systems under sparse sensor attacks: a set cover approach," *IEEE Transactions on Automatic Control*, vol. 64, no. 9, pp. 3949–3955, 2019.

[32] M. Lv, W. Yu, Y. Lv, J. Cao, and W. Huang, "An integral sliding mode observer for CPS cyber security attack detection," *Chaos*, vol. 29, Article ID 043120, 2019.

[33] W. Ao, Y. Song, and C. Wen, "Adaptive cyber-physical system attack detection and reconstruction with application to power systems," *IET Control Theory & Applications*, vol. 10, no. 12, pp. 1458–1468, 2016.

[34] V. R. Palleti, Y. C. Tan, and L. Samavedham, "A mechanistic fault detection and isolation approach using Kalman filter to improve the security of cyber physical systems," *Journal of Process Control*, vol. 68, pp. 160–170, 2018.

[35] C. Yang, Y. Jiang, W. He, J. Na, Z. Li, and B. Xu, "Adaptive parameter estimation and control design for robot manipulators with finite-time convergence," *IEEE Transactions on Industrial Electronics*, vol. 65, no. 10, pp. 8112–8123, 2018.

[36] F. Aghili, "Constrained Lagrangian dynamics based on reduced quasi-velocities and quasi-forces," *Multibody System Dynamics*, vol. 53, no. 4, pp. 327–343, 2021.

[37] V. Bloch, A. Degani, and A. Bechar, "A methodology of orchard architecture design for an optimal harvesting robot," *Biosystems Engineering*, vol. 166, pp. 126–137, 2018.

[38] W. Ren, S. Komada, K. Yubai, and S. Guo, "Zonotopic interval estimation for discrete-time Takagi-Sugeno fuzzy systems with a delayed nonquadratic framework," *Journal of the Franklin Institute*, vol. 359, no. 8, pp. 3883–3909, 2022.

[39] W. Ren, S. Komada, K. Yubai, and D. Yashiro, "Zonotopic kalman observer based sensor fault estimation for discrete-time takagi-sugeno fuzzy systems," in *Proceedings of the IEEE 17th International Conference on Advanced Motion Control (AMC)*, Padova, Italy, February 2022.